Extracellular vesicles from human liver stem cells inhibit tumor angiogenesis

Extracellular vesicles from human liver stem cells inhibit tumor angiogenesis.

Tatiana Lopatina
University of Turin, Department of Medical Sciences
Cristina Grange
University of Turin, Department of Medical Sciences
Valentina Fonsato
2i3T, Società per la gestione dell'incubatore di imprese e per il trasferimento tecnologico, Scarl, University of Turin
Marta Tapparo
University of Turin, Department of Medical Sciences
Alessia Brossa
University of Turin, Department of Molecular Biotechnology and Health Sciences
Sofia Fallo
University of Turin, Department of Medical Sciences
Adriana Pitino
University of Turin, Department of Medical Sciences
Maria Beatriz Herrera-Sanchez
2i3T, Società per la gestione dell'incubatore di imprese e per il trasferimento tecnologico, Scarl, University of Turin
Sharad Kholia
University of Turin, Department of Medical Sciences
Giovanni Camussi
University of Turin, Department of Medical Sciences
Benedetta Bussolati*
University of Turin, Department of Molecular Biotechnology and Health Sciences

*corresponding author: Benedetta Bussolati, Molecular Biotechnology Centre, University of Torino, via Nizza 52, 10126 Torino, Italy. Tel. 011-6706453, Fax. 011-6631184, e-mail: benedetta.bussolati@unito.it.

Running title: HLSC-EVs inhibit tumor angiogenesis

Abstract

Human liver stem-like cells (HLSC) and derived extracellular vesicles (EVs) were previously shown to exhibit anti-tumor activity. In the present study, we investigated whether HLSC-derived EVs (HLSC-EVs) were able to inhibit tumor angiogenesis *in vitro* and *in vivo*, in comparison with EVs derived from mesenchymal stem cells (MSC-EVs). The results obtained indicated that HLSC-EVs but not MSC-EVs inhibited the angiogenic properties of tumor-derived endothelial cells (TEC) both *in vitro* and *in vivo* in a model of subcutaneous implantation in Matrigel. Treatment of TEC with HLSC-EVs led to the down-regulation of pro-angiogenic genes. Since HLSC-EVs carry a specific set of microRNAs (miRNAs) that could target these genes, we investigated their potential role by transfecting TEC with HLSC-EV specific miRNAs. We observed that four miRNAs, namely miR-15a, miR-181b, miR-320c, and miR-874, significantly inhibited the angiogenic properties of TEC *in vitro*, and decreased the expression of their target genes (ITGB3, FGF1, EPHB4, PLAU). In parallel, TEC treated with HLSC-EVs significantly enhanced expression of miR-15a, miR-181b, miR-320c, and miR-874 associated with the down-regulation of FGF1 and PLAU. In summary, HLSC-EVs possess an anti-tumorigenic effect, based on their ability to inhibit tumor angiogenesis.

KEYWORDS:

Renal tumor endothelial cells, human liver stem cells, extracellular vesicles, microRNA, tumor angiogenesis, exosomes.

INTRODUCTION

Tumor vascularization is a fundamental step in tumor growth and metastasis. Solid tumors are in fact unable to grow more than a few millimetres per square in the absence of a vascular supply of oxygen and nutrients. Moreover, the number of metastases was reported to correlate with the vessel density of the primary tumor [1]. Tumor endothelial cells (TEC) are distinct from normal endothelial cells and display a pro-angiogenic phenotype [2, 3]. For instance, TEC demonstrate a higher *in vitro* motility and proliferation independent from serum and enhanced survival through Akt signaling [4]. From a phenotypic point of view, TEC have an altered expression of growth factors and their receptors, including VEGF and EGF receptors [5], integrins [6, 7], and extracellular matrix proteins [8]. TEC are also resistant to chemotherapeutic drugs and less sensitive to anti-angiogenic drugs targeting VEGF [9-11]. Furthermore, TEC genetically differ from normal endothelial cells [12-14].

Extracellular vesicles (EVs) are an important mechanism for cell-to-cell communication, and their active cargo may reprogram recipient cells, modifying their function and phenotype [15]. In fact, the activity of EVs seems to rely on the transfer of a number of different factors, including proteins, RNA, DNA, and lipids [16-18]. Stem cell-derived EVs and in particular human bone marrow-derived mesenchymal stromal cells (MSC) have been shown to display both pro-tumorigenic and anti-tumorigenic activities, depending on the tumor type and stage of development. In analogy, MSC-EVs may also modulate tumor vascularization in a positive or negative manner. For instance, MSC-EVs were reported to be pro-angiogenic after *in vivo* administration into tumor-bearing mice [19, 20]. Other studies [21-23] detected an indirect inhibitory effect of MSC-EVs on VEGF secretion by tumor cells. The mechanisms of this inhibition have been suggested to be due to the VEGF-targeting effect of miR-16 [21] and the down-regulation of PDGF/PDGFR axis [22].

Recently, we showed that the human liver stem-like cells (HLSC), another source of human resident mesenchymal stromal cells isolated from the liver [24], may display anti-tumor effects. In

particular, HLSC-EVs decreased the growth and survival of a number of different tumors, such as hepatocellular carcinoma, lymphoblastoma and glioblastoma [25].

In this study, we aimed to investigate the effect of MSC-EVs and HLSC-EVs on TEC isolated from renal carcinomas. In addition, we analyzed the potential role of microRNAs (miRNAs), carried by EVs in their biological activity.

RESULTS

HLSC-EVs inhibit the angiogenic potential and migration of renal TEC *in vitro.*

Stimulation with HLSC-EVs significantly inhibited the angiogenic properties of human renal TEC *in vitro* in a dose-depended manner (Figure 1, A, B, D). At variance, MSC-EVs did not show pro- or anti-angiogenic effects on TEC (Figure 1, A, C, D). Both EVs did not change TEC viability (data not shown). We also evaluated the effect of MSC-EVs and HLSC-EVs on the motility of TEC through a wound-healing assay. Both EVs significantly inhibited the migration of TEC at the dose of 10×10^3 EVs per TEC. However, HLSC-EVs were already effective at the lower dose of 1×10^3 EVs per TEC (Figure 1, E) compared to MSC-EVs.

As control experiments, we evaluated the effect of MSC-EVs and HLSC-EVs on normal endothelial cells: MSC-EVs were able to enhance the angiogenic property of human microvascular endothelial cells (HMECs), in line with their reported pro-angiogenic activity [26], whereas HLSC-EVs did not show any effect (Figure 1, F). This indicates that EVs from MSC and HLSC have different action on normal and tumor angiogenesis.

HLSC-EVs prevent tumor angiogenesis *in vivo.*

We subsequently evaluated the effect of MSC-EVs and HLSC-EVs *in vivo* by using a model of human tumor angiogenesis induced by TEC implanted subcutaneously in SCID mice within Matrigel [4]. In this model, TEC organize in patent structures connected with the mouse circulation within 7 days. In a pre-treatment setting, TEC were incubated with HLSC-EVs or MSC-EVs for 24 hours and implanted subcutaneously into SCID mice. Seven days after implantation, Matrigel plugs were excised and vessel density analyzed by trichrome staining. The analysis of control plugs showed, as expected, the presence of erythrocyte containing vessels (Figure 2, A). Plugs of TEC treated with HLSC-EVs for 24 hours before implantation did not present vessels (Figure 2 B, D), whereas those treated with MSC-EVs were highly angiogenic (Figure 2 C, D).

To evaluate whether EVs were able to affect formed tumor vessels, HLSC-EVs or MSC-EVs were injected at day 3 and 7 in Matrigel plugs containing an established TEC network. Plugs were explanted at day 10. The treatment with HLSC-EVs significantly reduced vessel density with respect to control and to treatment with MSC-EVs (Figure 2, E), confirming the *in vitro* results.

Molecular effects of HLSC-EVs on TEC

Based on these results, a molecular analysis of the changes occurring in TEC after HLSC-EVs stimulation during *in vitro* vessel-like structure organization was conducted using an Angiogenesis PCR array. Briefly, TEC were treated with HLSC-EVs (10×10^3 EVs/TEC) during *in vitro* angiogenesis and subsequently harvested for the PCR array. Among the 84 genes tested, we identified 11 pro-angiogenic factors significantly down-regulated in TEC treated with HLSC-EVs *in vitro* (Figure 3, A). In particular, HLSC-EVs down-regulated pro-angiogenic surface receptors including Tie-1, beta 3 integrin (ITGB3), ephrin receptor B4 (EPHB4) and endoglin (or CD105), as well as growth factors such as fibroblast growth factor 1 (FGF1), TGF family members, urokinase-type plasminogen activator (PLAU) and tissue factor (F3). Additionally, Akt1, known to be involved in the pro-angiogenic effects of TEC [27], was also down-regulated.

Identification of anti-angiogenic miRNAs carried by HLSC-EVs

To dissect the possible effectors of the observed gene regulation, we focused on miRNA content of HLSC-EVs. In order to accomplish this, we performed a bioinformatic analysis, followed by *in vitro* functional validation.

Using Funrich V3 software [28], we predicted miRNAs that target the 11 down-regulated genes. We identified 136 miRNAs and we matched them with miRNAs carried by HLSC-EVs. Among them, we identified 42 miRNAs expressed by HLSC-EVs (Figure 3, B). A subsequent analysis was performed to exclude those also present in MSC-EVs [29], due to their lacking effect on TEC (Figure 3, C). The complete list of HLSC- and MSC-EV microRNAs can be found in the exocarta repository (http://exocarta.org, number under request). Sixteen out of 42 miRNAs targeting the

identified genes were identified to be present only in HLSC-EVs and were adopted for further functional studies (Figure 3, D). Among them, three described as pro-tumorigenic (has-miR-30e-5p, has-miR-301a-3p, has-miR-212-3p) [30-32] were excluded. Therefore, we took in consideration 8 miRNAs: miR-15a, miR-20b, miR-23a, miR-93, miR-181b, miR-320c, miR-424, and miR-874 (Figure 3, D, in bold). Of importance, these selected miRNAs were expressed in low-level in the control TEC (Ct>33).

Effect of HLSC-EV miRNAs on TEC angiogenesis

To demonstrate the specificity of these selected miRNAs on the angiogenic properties of TEC, we transfected cells with the corresponding miRNA mimics. Two days after transfection, angiogenesis *in vitro* assay was performed. Four miRNAs (miR-15a, miR-181b, miR-320c and miR-874) significantly inhibited *in vitro* vessel-like structure formation (Figure 4, A), whereas miR-20b, miR-23a, miR-93, and miR-424 had no effect. Furthermore, all mimics had no effect on proliferation or apoptosis (Figure 4, B and C).

The next step was to investigate changes in the predicted targets' expression induced by the transfection with the four active miRNA mimics. The results showed a significant down-regulation of EPHB4, ITGB3, FGF1, and PLAU (Table 1, Figure 5).

In parallel, we evaluated the effective transfer of these miRNAs by HLSC-EVs in TEC. After 24 h incubation, these miRNAs, that had low basal expression in untreated cells, were significantly up-regulated (Figure 6, A), therefore validating ours *in silico* data. In parallel, we evaluated the effect of HLSC-EVs on the four genes found to be targets of the mimics (EPHB4, ITGB3, FGF1, and PLAU). We confirmed at both mRNA and protein level the down-regulation of FGF1 and PLAU in TEC treated with HLSC-EVs (Figure 6, B, C, and D).

DISCUSSION

In the present study, we found that EVs from a stromal stem cell population obtained from the human liver inhibited migration of tumor endothelial cells, and significantly reduced vessel-like formation *in vitro*. Experiments performed *in vivo* in a model of tumor angiogenesis in SCID mice also showed that HLSC-EVs were able to inhibit vessel formation and growth. This effect appeared to be specific to HLSC-EVs as bone marrow-derived MSC-EVs did not display any effect. In addition, this anti-angiogenic feature of HLSC-EVs was dependent on the presence of a specific miRNA subset.

Tumor angiogenesis has different characteristics and mechanisms in respect to normal angiogenesis. TEC derived from renal carcinoma were shown to be able to form *in vivo* a human vascular network connected with mouse vasculature once implanted within Matrigel in mice [2, 4]. These cells maintain a pro-angiogenic program in an autocrine manner [2, 4]. Several studies have previously shown that endothelial cells derived from different tumors are different from the normal endothelium as they express a distinct and unique molecular and functional phenotype [2, 33]. EVs released from stem cells were shown to be able to reprogram target cells by inducing epigenetic changes [34, 35]. This observation prompted us to investigate whether EVs derived from MSC and HLSC were able to modify the pro-angiogenic phenotype of TEC.

Previous studies of the effect of MSC and MSC-derived EVs provided conflicting results on *in vivo* tumor growth [19, 21, 36]. These contradictory results probably depend on cell growth conditions and on timing of administration [37-39]. MSC-EVs are described as strictly pro-angiogenic for healthy endothelial cells [40, 41]. Lindoso *et al*. showed that EVs derived from MSC primed by tumor cells acquired a pro-angiogenic and pro-tumorigenic activity [42]. In the present study, we found that MSC-EVs were able to inhibit migration but not influence proliferation and angiogenesis of TEC. Pre-treatment of TEC with MSC-EVs was unable to modify the formation of an *in vivo* vascular

network by TEC. In contrast to MSC-EVs, HLSC-EVs were found to possess an intrinsic anti-angiogenic activity. Previous studies have shown that HLSC-EVs inhibited tumor growth both *in vitro* and *in vivo* and the mechanism was related to the delivery of anti-tumor miRNAs that were able to down-regulate oncogenic targets [25]. Herein, we have found that HLSC-EVs were able to almost completely abrogate tumor angiogenesis *in vitro* and *in vivo* without affecting normal endothelial cells.

EVs are complex structures composed of specific functional proteins, lipids, and nucleic acids. The biological activity of EVs depends on the coordinated action of all these components. However, a number of reports have indicated the relevant role of EV mediated miRNA transfer in inducing epigenetic changes in target cells. In the present study, we identified four miRNAs carried by HLSC-EVs but not by MSC-EVs with an anti-angiogenic function. These miRNAs, miR-15a, mir-181b, miR-320c, and miR-874, were able to inhibit tumor angiogenesis when transfected in TEC mainly by down-regulating the expression of their target genes (FGF1, PLAU, ITGB3, and EPHB4). In parallel, when TEC were stimulated with HLSC-EVs, a significantly enhanced expression of these miRNAs was observed. The effective down-regulation of the predicted target genes was observed only for FGF1 and PLAU. These miRNAs were previously described to have different function in tumors. MiR-15a is a well-known tumor suppressor. This miRNA inhibits cell proliferation, promotes apoptosis of cancer cells, and suppresses tumor growth by targeting multiple oncogenes, including BCL2, MCL1, CCND1, and WNT3A [43]. MiR-181b could play a contradictory role in tumor development depending on the type of tumor and cell being studied [44]. Mir-874 is described not only as a tumor suppressor [45-47] but also as an inhibitor of tumor angiogenesis through STAT3/VEGF-A pathway [48]. miR-320c, on the other hand, has been shown to be down-regulated in many types of cancer, such as myeloma [49], colorectal cancer [50], and bladder cancer [51]. Predicted targets that we have found by the Funrich online software for every miRNA have not been previously described or confirmed, except for EPHB4 as a target for miR-

181 [52]. After the transfection of TEC with the selected miRNAs or stimulation with HLSC-EVs, two predicted pro-angiogenic genes were significantly down-regulated at mRNA and protein level. FGF1 is one of the most important pro-angiogenic factor involved in tumor angiogenesis [53, 54]. FGF1 is able to regulate angiogenesis independently from VEGF [55] and an enhanced expression of this factor has been reported in different types of tumors [56, 57]. PLAU is a gene that codes for urokinase-type plasminogen activator (uPA), an enzyme that activates plasmin from plasminogen. Plasmin participates in the proteolytic processes of extracellular matrix degradation which is important for angiogenesis and cancer progression [58]. FGF1 and PLAU are connected through the receptors of FGF1 (FGFRs) that could activate uPA and enhance the expression of its receptor uPAR. Furthermore, FGF1, uPA, and uPAR are all linked through FGFRs creating a positive feedback loop. In fact, cells overexpressing FGFRs were shown to be more invasive and tumorigenic [59].

In conclusion, we have shown that HLSC-EVs specifically and significantly inhibit tumor angiogenesis *in vitro* and *in vivo*. Furthermore, based on the bioinformatic analysis and the characterization of anti-angiogenic miRNAs carried by HLSC-EVs, we postulate that EV mediated transfer of miRNAs may be involved in the inhibition of tumor angiogenesis through down-regulation of a number of genes including FGF1 and PLAU.

MATERIALS AND METHODS

Cell cultures

TEC have been previously isolated and cultured in our laboratory from surgical specimens of patients with renal carcinomas [4]. TEC were isolated from digested tissue using anti-CD105 positive selection by magnetic cell sorting (MACS system, Miltenyi Biotech) and grown in EndoGro complete medium (Millipore), as described previously [4].

HLSC were isolated in our laboratory from human cryopreserved normal hepatocytes obtained from Lonza as described previously [24]. Briefly, cells were plated in hepatocyte serum-free medium (Gibco Hepatozyme-SFM; Invitrogen) at a density of $1.0–1.5\times10^5$ viable cells per cm^2 on collagen-coated culture plates for 2 weeks. After 2 weeks of culture, the medium was substituted to α -minimum essential medium/endothelial cell basal medium-1 (α-MEM/EBM) (3:1) (Gibco/Euroclone) supplemented with L-glutamine (5 mM), Hepes (12 mM, pH7.4), penicillin (50 IU/ml), streptomycin (50 µg/ml), (all from Sigma), and 10 % FBS (Lonza). At this moment, individually attached cells were cloned after 3 weeks and expanded. HLSC were positive for CD73, CD90, CD29, and CD44 and negative for CD45, CD34, CD117 (c-kit), and CD133.

MSC were purchased from Lonza and cultured in MSCBM complete medium (Lonza).

EV isolation and characterization

Isolation of EVs was performed as described previously [60] with minor modifications. Briefly, confluent HLSC or MSC were cultured in serum-free RPMI FBS free for 18 hours. Post culture, the medium was centrifuged for 30 minutes at 3000g to remove cell debris and apoptotic bodies. After which, the supernatant was ultracentrifuged for 2 hours at 100.000g, 4°C using the Beckman Coulter Optima L-100K Ultracentrifuge with the rotor type 45 Ti 45000RPM. The pellet of EVs obtained was resuspended in RPMI supplemented with 10 % of DMSO. Suspension of HLSC-EVs

was then stored at -80°C until further use. EVs were analyzed using NTA analysis and electron microscopy. Mean size of EVs was 90 nm (± 20) (Supplementary figure).

Viability and migration tests

For the proliferation test, TEC were seeded in a 96 well plate at the density of 2×10^3/well. The next day, cells were treated with HLSC-EVs or MSC-EVs at the concentrations of 1×10^3, or 5×10^3, or 10×10^3 EVs per TEC in EndoGro complete medium (Lonza). Proliferation was measured by BrdU incorporation at 24, 48 and 72 hours post EVs stimulation using Cell Proliferation ELISA, BrdU (colorimetric) kit (Roche, 11647229001) according to the manufacturer's instructions. For the migration test, TEC were seeded in a 24-well plate and grown to confluence. EVs were then added in the concentrations of 1×10^{15}, or 5×10^{15}, or 10×10^{15} EVs/well just after the scratch was done. Images were captured using a light microscope with the magnification of 10× at the time points of 0, 3, 7 and 24 hours after the scratch. The distance was measured by LAS software (Leica) and, the results expressed as mean ± SEM of three independent experiments.

Vessel-like structure formation *in vitro*

TEC were seeded onto Matrigel-coated 24-well plates at the density of 25×10^3 cells per well and cultured in EndoGro complete medium in the presence of 1×10^3, 5×10^3, 10×10^3 or 20×10^3 EVs per TEC. TEC without EVs served as a control. After incubating for 24 h, phase-contrast images (magnification, 10×) were recorded and the total length of the network structures was measured using LAS software (Leica). The total length per field was calculated in five random fields and expressed as a ratio respective to the control. Data were expressed as mean ± SEM.

In vivo angiogenesis model

Animal studies were conducted in accordance with the national guidelines and regulations and were approved by the Ethics Committee of the University of Torino (Protocol Number: 338/2016-PR). A model of *in vivo* tumor angiogenesis obtained by TEC the injection of Matrigel

incorporated with TEC was used to assess the effect of stem cell-derived EVs, as described previously [4]. To prevent the development of tumor angiogenesis TEC were pre-treated before injecting. For this purpose SCID mice (6-8 weeks old) (Charles River Laboratories) were subcutaneously injected with 1×10^6 TEC incorporated within Matrigel, pre-treated or not with HLSC-EVs/MSC-EVs (10×10^3 EV per cell): (n=8 each group). After 7 days, Matrigel plugs were excised and vessel density was analyzed by Masson's trichromic reaction staining. To evaluate the influence of EVs on established tumor vessels, Matrigel incorporated with 1×10^6 TEC was subcutaneously injected in SCID mice. HLSC-EVs or MSC-EVs (10×10^3 EVs per cell or 1×10^{10} EVs per plug) were injected twice into Matrigel plugs on day 3 and 7 post injection. Control mice were injected with the vehicle (PBS). At day 10 of the experiment, mice were sacrificed and Matrigel plugs excised for histochemical analysis (n=8 for each group).

Gene expression study and Real-time PCR

miRNA expression levels in HLSC-EVs or MSC-EVs were evaluated using the Applied Biosystems TaqMan® Array Human MicroRNA A/B Cards (Applied Biosystems, Foster City, CA) to profile 754 mature miRNAs by qRT-PCR. The kit used miRNA-specific stem-loop reverse transcription primers and TaqMan probes to detect mature miRNA transcripts in a 2-step real-time reverse-transcription PCR assay. Briefly, single-stranded cDNA was generated from total RNA sample (80 ng) by reverse transcription using a mixture of looped primers (Multiplex RT kit, Applied Biosystems) following the manufacturer's protocol. The RT reactions were then diluted and mixed with a Taqman universal master Mix (Applied) in a ratio of 1:1, and loaded in the TaqMan microfluid card to analyze via qRT-PCR. All reactions were performed using an Applied Biosystems 7900HT real-time PCR instrument equipped with a 384 well reaction plate. Raw Ct values were calculated using the SDS software version 2.3 using automatic baseline and threshold. We analyzed the expression of miRNAs in 3 replicate samples of HLSC-EVs. All miRNAs that

were amplified after 35 cycles of PCR were classified as unexpressed. Furthermore, only miRNAs that were detected or undetected in more than two replicate samples were taken into consideration.

qRT-PCR was used to confirm miRNAs or target gene expression in TEC. Briefly, 200 ng of input RNA from all samples were reverse transcribed with the miScript Reverse Transcription Kit and the cDNA was then used to detect and quantify miRNAs or genes of interest by qRT-PCR using the miScript SYBR Green PCR Kit (all from Qiagen). All samples were run in triplicate using 3 ng of cDNA for each reaction as described by the manufacturer's protocol (Qiagen). Relative expression data were then normalized using the mean expression value, calculated on the overall miRNA expression in each array, according to a Ct detection cut-off of 35 PCR cycles as described by Mestdagh et al. [61].

PCR analysis of the expression of pro-angiogenic genes in TEC, treated or not with HLSC-EVs, was done using Human Angiogenesis PCR Array (RT^2 Profiler PCR array, 96/well Format, Qiagen) in triplicate according to the manufacturers' instructions. Data were analyzed using SaBioscience (Qiagen) online software and expressed as Relative Quantification ± CI (Confidence interval). To compare the list of genes down-regulated in TEC after HLSC-EVs stimulation (miRNAs carried by these EVs) the online software FunRich (http://funrich.org) was used.

Cell transfection

Transfection of TEC was performed using HiPerfect reagent (Qiagen). To identify the optimal concentration for transfection, TEC were transfected with a scramble control RNA marked with FITC. FACS analysis performed the day after transfection, revealed that more than 60 % of TEC were transfected with no damage on their viability and proliferation.

Transfection of TEC was performed using the following mimic miRNAs: miR-15a, miR-20b, miR-23a, miR-93, miR-181b, miR-320c, miR-424, and miR-874 (all from Qiagen). The day after transfection fresh growth medium was replaced and at day two the cells were used for *in vitro*

experiments (proliferation, apoptosis tests, angiogenesis in vitro assay) or gene expression analysis (Real-time PCR, Western blot, FACS analysis).

Fluorescence-activated cell sorting (FACS) analysis

FACS analysis of HLSC-EVs and MSC-EVs was performed using CytoFLEX Flow Cytometer (Beckman Coulter) (Supplementary figure). Antibodies used were: the FITC- conjugated antibodies anti CD63 (Abnova), anti CD105 (Dako Cytomation), anti CD90 (BD Pharmigen), anti CD44 (Miltenyi Biotech), CD45 (BD Pharmigen), anti ICAM and anti VCAM (Serotec), CD31 (BioLegend), integrin subunit α4, α5, α6 (from BD Pharmigen); PE- conjugated antibodies anti CD73 (BD Pharmigen), anti integrin subunit α4, α5 (all from BD Pharmigen) and VE-cadherin (BioLegend). FITC or PE mouse non-immune isotypic IgG (Dako Cytomation) were used as a control.

Western blot

Protein samples were separated by 4% to 15% gradient sodium dodecyl sulfate–polyacrylamide gel electrophoresis (SDS PAGE) and subjected to immunoblotting with antibodies to PLAU (Abcam, ab131433) or FGF1 (Abcam ab9588). The protein bands were visualized with an enhanced chemiluminescence detection kit and ChemiDoc™ XRS+ System (BioRad). Cell lysates (20 µg protein) were loaded per well.

Statistics

Data were assessed for normality of distribution using the Kolmogorov-Smirnov test. Statistical analysis was performed using SigmaPlot 11.0 Software. Differences between treatment and control groups were then analyzed using Dunnett's test when the distribution was normal. Data are expressed as mean ± SEM. We considered differences to be significant when $p<0.05$.

Conflict of interest

T.L., B.B., and G.C. are named as inventors in a related patent application # 170095.

.

Acknowledgments

This work was supported by Associazione Italiana per la Ricerca sul Cancro (AIRC, Project IG2015 # 16973) to B.B. and G.C. and by grant No. 071215 from Unicyte A.G. to GC and B.B.

References:

1. Liotta LA, Saidel MG, Kleinerman J. The significance of hematogenous tumor cell clumps in the metastatic process. *Cancer research* 1976; **36**(3): 889-94.
2. Bussolati B, Grange C, Camussi G. Tumor exploits alternative strategies to achieve vascularization. *FASEB journal : official publication of the Federation of American Societies for Experimental Biology* 2011; **25**(9): 2874-82.
3. Dudley AC. Tumor endothelial cells. *Cold Spring Harbor perspectives in medicine* 2012; **2**(3): a006536.
4. Bussolati B, Deambrosis I, Russo S, Deregibus MC, Camussi G. Altered angiogenesis and survival in human tumor-derived endothelial cells. *FASEB journal : official publication of the Federation of American Societies for Experimental Biology* 2003; **17**(9): 1159-61.
5. Hida K, Hida Y, Shindoh M. Understanding tumor endothelial cell abnormalities to develop ideal anti-angiogenic therapies. *Cancer science* 2008; **99**(3): 459-66.
6. Goel HL, Moro L, Murphy-Ullrich JE, Hsieh CC, Wu CL, Jiang Z*, et al.* Beta1 integrin cytoplasmic variants differentially regulate expression of the antiangiogenic extracellular matrix protein thrombospondin 1. *Cancer research* 2009; **69**(13): 5374-82.
7. Sayeed A, Fedele C, Trerotola M, Ganguly KK, Languino LR. IGF-IR promotes prostate cancer growth by stabilizing alpha5beta1 integrin protein levels. *PloS one* 2013; **8**(10): e76513.
8. Dutta A, Li J, Lu H, Akech J, Pratap J, Wang T*, et al.* Integrin alphavbeta6 promotes an osteolytic program in cancer cells by upregulating MMP2. *Cancer research* 2014; **74**(5): 1598-608.
9. Akiyama K, Ohga N, Hida Y, Kawamoto T, Sadamoto Y, Ishikawa S*, et al.* Tumor endothelial cells acquire drug resistance by MDR1 up-regulation via VEGF signaling in tumor microenvironment. *The American journal of pathology* 2012; **180**(3): 1283-93.
10. Brossa A, Grange C, Mancuso L, Annaratone L, Satolli MA, Mazzone M*, et al.* Sunitinib but not VEGF blockade inhibits cancer stem cell endothelial differentiation. *Oncotarget* 2015; **6**(13): 11295-309.
11. Fiorio Pla A, Brossa A, Bernardini M, Genova T, Grolez G, Villers A*, et al.* Differential sensitivity of prostate tumor derived endothelial cells to sorafenib and sunitinib. *BMC cancer* 2014; **14**: 939.
12. Akino T, Hida K, Hida Y, Tsuchiya K, Freedman D, Muraki C*, et al.* Cytogenetic abnormalities of tumor-associated endothelial cells in human malignant tumors. *The American journal of pathology* 2009; **175**(6): 2657-67.
13. Maishi N, Ohba Y, Akiyama K, Ohga N, Hamada J, Nagao-Kitamoto H*, et al.* Tumour endothelial cells in high metastatic tumours promote metastasis via epigenetic dysregulation of biglycan. *Scientific reports* 2016; **6**: 28039.
14. Pezzolo A, Parodi F, Corrias MV, Cinti R, Gambini C, Pistoia V. Tumor origin of endothelial cells in human neuroblastoma. *Journal of clinical oncology : official journal of the American Society of Clinical Oncology* 2007; **25**(4): 376-83.
15. Lopatina T. Cross Talk between Cancer and Mesenchymal Stem Cells through Extracellular Vesicles Carrying Nucleic Acids. *Frontiers of Oncology* 2016; **6**.
16. Ratajczak MZ, Ratajczak J. Extracellular Microvesicles as Game Changers in Better Understanding the Complexity of Cellular Interactions-From Bench to Clinical Applications. *The American journal of the medical sciences* 2017; **354**(5): 449-52.

17. DeRita RM, Zerlanko B, Singh A, Lu H, Iozzo RV, Benovic JL*, et al.* c-Src, Insulin-Like Growth Factor I Receptor, G-Protein-Coupled Receptor Kinases and Focal Adhesion Kinase are Enriched Into Prostate Cancer Cell Exosomes. *Journal of cellular biochemistry* 2017; **118**(1): 66-73.
18. Quesenberry PJ, Goldberg LR, Aliotta JM, Dooner MS, Pereira MG, Wen S*, et al.* Cellular phenotype and extracellular vesicles: basic and clinical considerations. *Stem cells and development* 2014; **23**(13): 1429-36.
19. Zhu W, Huang L, Li Y, Zhang X, Gu J, Yan Y*, et al.* Exosomes derived from human bone marrow mesenchymal stem cells promote tumor growth in vivo. *Cancer letters* 2012; **315**(1): 28-37.
20. Zhu W, Xu W, Jiang R, Qian H, Chen M, Hu J*, et al.* Mesenchymal stem cells derived from bone marrow favor tumor cell growth in vivo. *Exp Mol Pathol* 2006; **80**(3): 267-74.
21. Lee JK, Park SR, Jung BK, Jeon YK, Lee YS, Kim MK*, et al.* Exosomes derived from mesenchymal stem cells suppress angiogenesis by down-regulating VEGF expression in breast cancer cells. *PloS one* 2013; **8**(12): e84256.
22. Ho IA, Toh HC, Ng WH, Teo YL, Guo CM, Hui KM*, et al.* Human bone marrow-derived mesenchymal stem cells suppress human glioma growth through inhibition of angiogenesis. *Stem cells* 2013; **31**(1): 146-55.
23. Alcayaga-Miranda F, Gonzalez PL, Lopez-Verrilli A, Varas-Godoy M, Aguila-Diaz C, Contreras L*, et al.* Prostate tumor-induced angiogenesis is blocked by exosomes derived from menstrual stem cells through the inhibition of reactive oxygen species. *Oncotarget* 2016; **7**(28): 44462-77.
24. Herrera MB, Bruno S, Buttiglieri S, Tetta C, Gatti S, Deregibus MC*, et al.* Isolation and characterization of a stem cell population from adult human liver. *Stem cells* 2006; **24**(12): 2840-50.
25. Fonsato V, Collino F, Herrera MB, Cavallari C, Deregibus MC, Cisterna B*, et al.* Human liver stem cell-derived microvesicles inhibit hepatoma growth in SCID mice by delivering antitumor microRNAs. *Stem cells* 2012; **30**(9): 1985-98.
26. Bronckaers A, Hilkens P, Martens W, Gervois P, Ratajczak J, Struys T*, et al.* Mesenchymal stem/stromal cells as a pharmacological and therapeutic approach to accelerate angiogenesis. *Pharmacology & therapeutics* 2014; **143**(2): 181-96.
27. Bussolati B, Assenzio B, Deregibus MC, Camussi G. The proangiogenic phenotype of human tumor-derived endothelial cells depends on thrombospondin-1 downregulation via phosphatidylinositol 3-kinase/Akt pathway. *Journal of molecular medicine* 2006; **84**(10): 852-63.
28. Pathan M, Keerthikumar S, Ang CS, Gangoda L, Quek CY, Williamson NA*, et al.* FunRich: An open access standalone functional enrichment and interaction network analysis tool. *Proteomics* 2015; **15**(15): 2597-601.
29. Collino F, Bruno S, Incarnato D, Dettori D, Neri F, Provero P*, et al.* AKI Recovery Induced by Mesenchymal Stromal Cell-Derived Extracellular Vesicles Carrying MicroRNAs. *Journal of the American Society of Nephrology : JASN* 2015; **26**(10): 2349-60.
30. Yu F, Deng H, Yao H, Liu Q, Su F, Song E. Mir-30 reduction maintains self-renewal and inhibits apoptosis in breast tumor-initiating cells. *Oncogene* 2010; **29**(29): 4194-204.
31. Liang B, Yin JJ, Zhan XR. MiR-301a promotes cell proliferation by directly targeting TIMP2 in multiple myeloma. *International journal of clinical and experimental pathology* 2015; **8**(8): 9168-74.

32. Ma C, Nong K, Wu B, Dong B, Bai Y, Zhu H*, et al.* miR-212 promotes pancreatic cancer cell growth and invasion by targeting the hedgehog signaling pathway receptor patched-1. *Journal of experimental & clinical cancer research : CR* 2014; **33**: 54.
33. Streubel B, Chott A, Huber D, Exner M, Jager U, Wagner O*, et al.* Lymphoma-specific genetic aberrations in microvascular endothelial cells in B-cell lymphomas. *The New England journal of medicine* 2004; **351**(3): 250-9.
34. Ratajczak J, Wysoczynski M, Hayek F, Janowska-Wieczorek A, Ratajczak MZ. Membrane-derived microvesicles: important and underappreciated mediators of cell-to-cell communication. *Leukemia* 2006; **20**(9): 1487-95.
35. Deregibus MC, Cantaluppi V, Calogero R, Lo Iacono M, Tetta C, Biancone L*, et al.* Endothelial progenitor cell derived microvesicles activate an angiogenic program in endothelial cells by a horizontal transfer of mRNA. *Blood* 2007; **110**(7): 2440-8.
36. Katakowski M, Buller B, Zheng X, Lu Y, Rogers T, Osobamiro O*, et al.* Exosomes from marrow stromal cells expressing miR-146b inhibit glioma growth. *Cancer letters* 2013; **335**(1): 201-4.
37. Lopatina T, Gai C, Deregibus MC, Kholia S, Camussi G. Cross Talk between Cancer and Mesenchymal Stem Cells through Extracellular Vesicles Carrying Nucleic Acids. *Frontiers in oncology* 2016; **6**: 125.
38. Chang AI, Schwertschkow AH, Nolta JA, Wu J. Involvement of mesenchymal stem cells in cancer progression and metastases. *Current cancer drug targets* 2015; **15**(2): 88-98.
39. Hong IS, Lee HY, Kang KS. Mesenchymal stem cells and cancer: friends or enemies? *Mutation research* 2014; **768**: 98-106.
40. Anderson JD, Johansson HJ, Graham CS, Vesterlund M, Pham MT, Bramlett CS*, et al.* Comprehensive Proteomic Analysis of Mesenchymal Stem Cell Exosomes Reveals Modulation of Angiogenesis via Nuclear Factor-KappaB Signaling. *Stem cells* 2016; **34**(3): 601-13.
41. Merino-Gonzalez C, Zuniga FA, Escudero C, Ormazabal V, Reyes C, Nova-Lamperti E*, et al.* Mesenchymal Stem Cell-Derived Extracellular Vesicles Promote Angiogenesis: Potencial Clinical Application. *Frontiers in physiology* 2016; **7**: 24.
42. Lindoso RS, Collino F, Camussi G. Extracellular vesicles derived from renal cancer stem cells induce a pro-tumorigenic phenotype in mesenchymal stromal cells. *Oncotarget* 2015; **6**(10): 7959-69.
43. Aqeilan RI, Calin GA, Croce CM. miR-15a and miR-16-1 in cancer: discovery, function and future perspectives. *Cell death and differentiation* 2010; **17**(2): 215-20.
44. Liu J, Shi W, Wu C, Ju J, Jiang J. miR-181b as a key regulator of the oncogenic process and its clinical implications in cancer (Review). *Biomedical reports* 2014; **2**(1): 7-11.
45. Dong D, Gong Y, Zhang D, Bao H, Gu G. miR-874 suppresses the proliferation and metastasis of osteosarcoma by targeting E2F3. *Tumour biology : the journal of the International Society for Oncodevelopmental Biology and Medicine* 2016; **37**(5): 6447-55.
46. Jiang T, Guan LY, Ye YS, Liu HY, Li R. MiR-874 inhibits metastasis and epithelial-mesenchymal transition in hepatocellular carcinoma by targeting SOX12. *American journal of cancer research* 2017; **7**(6): 1310-21.
47. Zhao B, Dong AS. MiR-874 inhibits cell growth and induces apoptosis by targeting STAT3 in human colorectal cancer cells. *European review for medical and pharmacological sciences* 2016; **20**(2): 269-77.

48. Zhang X, Tang J, Zhi X, Xie K, Wang W, Li Z*, et al.* miR-874 functions as a tumor suppressor by inhibiting angiogenesis through STAT3/VEGF-A pathway in gastric cancer. *Oncotarget* 2015; **6**(3): 1605-17.
49. Alzrigat M, Jernberg-Wiklund H. The miR-125a and miR-320c are potential tumor suppressor microRNAs epigenetically silenced by the polycomb repressive complex 2 in multiple myeloma. *RNA & disease* 2017; **4**(2).
50. Vishnubalaji R, Hamam R, Yue S, Al-Obeed O, Kassem M, Liu FF*, et al.* MicroRNA-320 suppresses colorectal cancer by targeting SOX4, FOXM1, and FOXQ1. *Oncotarget* 2016; **7**(24): 35789-802.
51. Wang X, Wu J, Lin Y, Zhu Y, Xu X, Xu X*, et al.* MicroRNA-320c inhibits tumorous behaviors of bladder cancer by targeting Cyclin-dependent kinase 6. *Journal of experimental & clinical cancer research : CR* 2014; **33**: 69.
52. Foo CH, Rootes CL, Cowley K, Marsh GA, Gould CM, Deffrasnes C*, et al.* Dual microRNA Screens Reveal That the Immune-Responsive miR-181 Promotes Henipavirus Entry and Cell-Cell Fusion. *PLoS pathogens* 2016; **12**(10): e1005974.
53. Slavin J. Fibroblast growth factors: at the heart of angiogenesis. *Cell biology international* 1995; **19**(5): 431-44.
54. Raju R, Palapetta SM, Sandhya VK, Sahu A, Alipoor A, Balakrishnan L*, et al.* A Network Map of FGF-1/FGFR Signaling System. *Journal of signal transduction* 2014; **2014**: 962962.
55. Cao R, Brakenhielm E, Pawliuk R, Wariaro D, Post MJ, Wahlberg E*, et al.* Angiogenic synergism, vascular stability and improvement of hind-limb ischemia by a combination of PDGF-BB and FGF-2. *Nature medicine* 2003; **9**(5): 604-13.
56. Mori S, Tran V, Nishikawa K, Kaneda T, Hamada Y, Kawaguchi N*, et al.* A dominant-negative FGF1 mutant (the R50E mutant) suppresses tumorigenesis and angiogenesis. *PloS one* 2013; **8**(2): e57927.
57. Li J, Wei Z, Li H, Dang Q, Zhang Z, Wang L*, et al.* Clinicopathological significance of fibroblast growth factor 1 in non-small cell lung cancer. *Human pathology* 2015; **46**(12): 1821-8.
58. Tang L, Han X. The urokinase plasminogen activator system in breast cancer invasion and metastasis. *Biomedicine & pharmacotherapy = Biomedecine & pharmacotherapie* 2013; **67**(2): 179-82.
59. Billottet C, Janji B, Thiery JP, Jouanneau J. Rapid tumor development and potent vascularization are independent events in carcinoma producing FGF-1 or FGF-2. *Oncogene* 2002; **21**(53): 8128-39.
60. Herrera MB, Fonsato V, Gatti S, Deregibus MC, Sordi A, Cantarella D*, et al.* Human liver stem cell-derived microvesicles accelerate hepatic regeneration in hepatectomized rats. *Journal of cellular and molecular medicine* 2010; **14**(6B): 1605-18.
61. Mestdagh P, Van Vlierberghe P, De Weer A, Muth D, Westermann F, Speleman F*, et al.* A novel and universal method for microRNA RT-qPCR data normalization. *Genome biology* 2009; **10**(6): R64.

Table 1. Relative expression of pro-angiogenic genes in TEC, transfected with selected miRNAs, versus control TEC; in brackets, miRNAs that target the demonstrated genes.

Gene	RQ in transfected TEC vs. control TEC	Targeting miRNA
ITGB3	0.33	miR-320c
FGF1	0.39	miR-15a
EPHB4	0.39 0.48	miR-181b miR-874
PLAU	0.51	miR-181b

Figure legends:

Figure 1. The effect of HLSC-EVs or MSC-EVs on the angiogenic properties of TEC *in vitro.* Formation of vessel-like structures by control TEC (A), by TEC treated with HLSC-EVs (B) or with MSC-EVs (C); (D) diagram of the total length of vessel-like structures per field, formed by control TEC or TEC treated with different doses of EVs; (E) diagram of the TEC migration during wound healing assay in the presence or absence of different doses of EVs; (F) diagram of the total length of vessel-like structures per field, formed by HMEC, treated with different doses of EVs. Data are expressed as mean ± SEM of 3 experiments performed in duplicate. Statistical analysis was performed using Dunnett's test vs. control stimulated with vehicle alone. * - $p<0.05$.

Figure 2. Tumor angiogenesis *in vivo.* Representative images of Matrigel sections, stained with Masson's trichromic reaction (extracellular matrix is stained in blue, cells in red and erythrocytes in yellow): (A) Matrigel plugs containing control TEC treated with vehicle alone; (B) Matrigel plugs containing TEC, pre-treated with 10×10^3 HLSC-EVs per cell; (C) Matrigel plugs containing TEC, pre-treated with 10×10^3 MSC-EVs per cell. (Original magnification ×20; erythrocytes containing vessels are indicated by arrows). (D) Diagram of vessel density in Matrigel containing control TEC or TEC pre-treated with HLSC-EVs or MSC-EVs. (E) Diagram of vessel density in TEC contained Matrigel, injected or not with HLSC-EVs or MSC-EVs on day 3 and 7 after TEC injection. Data are expressed as mean ± SEM of 8 experiments performed independently. Statistical analysis was performed using Dunnett's test vs. control group stimulated with vehicle alone. * - $p<0.05$; ***- $p<0.001$.

Figure 3. Selection of miRNAs specific to HLSC-EVs responsible for the anti-angiogenic effect on TEC. (A) List of the genes down-regulated in TEC after treatment with HLSC-EVs (n=3

experiments; data are expressed as average Fold change ± CI (Confidence interval); these genes could be targeted by 136 miRNAs (B), 42 of which are carried by HLSC-EVs. Among these 42 miRNAs, 26 are also carried by MSC-EVs, which did not show any anti-angiogenic effect on TEC, therefore these 26 miRNAs were excluded from the study (C). Panel C shows 16 miRNAs specific to HLSC-EVs that could be relevant towards the biologic action of EVs on TEC. miRNAs selected for further studies are indicated in bold (D).

Figure 4. Influence of selected miRNAs transfected in TEC on their pro-angiogenic properties and viability. The diagrams show: (A) *in vitro* vessel-like structure formation by TEC transfected with selected mimic RNA or scramble RNA; (B) apoptosis rate of the transfected TEC; (C) proliferation rate of the transfected TEC. Data are expressed as mean ± SEM of 3 experiments performed independently. Statistical analysis was performed using Dunnett's test vs. control transfected with scramble RNA. * - $p<0.05$.

Figure 5. Expression of miRNAs and their targets in TEC, transfected with the selected mimic miRNAs. (A) expression of miR-15a and its target genes FGF1, EPHB4; (B) expression of miR-181b and its target genes PLAU, ITGB3, FGF1, EPHB4; (C) expression of miR-320c and its target genes PLAU, ITGB4, FGF1; (D) expression of miR-874 and its target genes EPHB4, PLAU, ITGB3, FGF1; Data are expressed as RQ mean ± SEM of 5 experiments performed. Statistical analysis was performed using Dunnett's test vs. control transfected with scramble RNA. * - $p<0.05$.

Figure 6. Expression of miRNAs and their targets in TEC treated with HLSC-EVs. (A) Relative expression of miRNAs in the control TEC and TEC treated with HLSC-EVs; (B) Relative expression of target genes in control TEC and TEC treated with HLSC-EVs; (C) Representative

image of Western blot analysis of the FGF1 expression in control TEC, TEC transfected with miR-15a or stimulated with HLSC-EVs. (D) Representative image of Western blots showing the expression of PLAU in control TEC, TEC transfected with miR-181b or stimulated with HLSC-EVs. Data are expressed as mean ± SEM of 6 experiments performed independently. Statistical analysis was performed using Dunnett's test vs. control TEC treated with vehicle alone; * - $p<0.05$.

Supplementary figure 1. Characterization of MSC- and HLSC-derived EVs.

(A) Representative image of NTA analysis of HLSC-EVs; (B) representative image of NTA analysis of MSC-EVs; (C) Representative electron microscopy image of HLSC-EVs, 100×, (black line, 400 nm); (D) – Representative electron microscopy image of HLSC-EVs, 100×, (black line, 400 nm); (E) – Surface marker expression of HLSC-EVs and MSC-EVs according to FACS analysis. Data are expressed as mean ± SEM of 3 experiments.

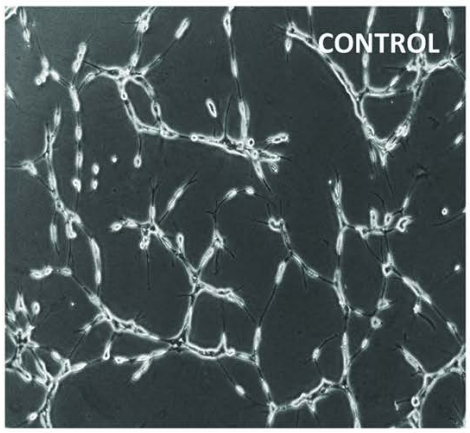

A

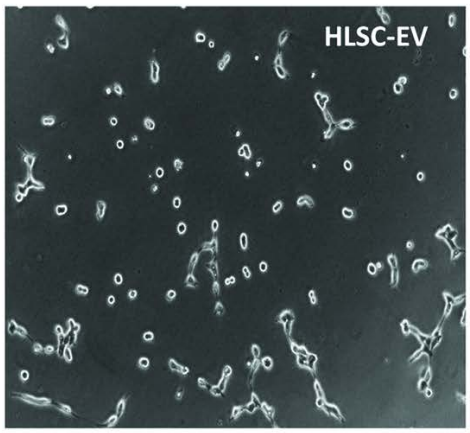

B

C

D

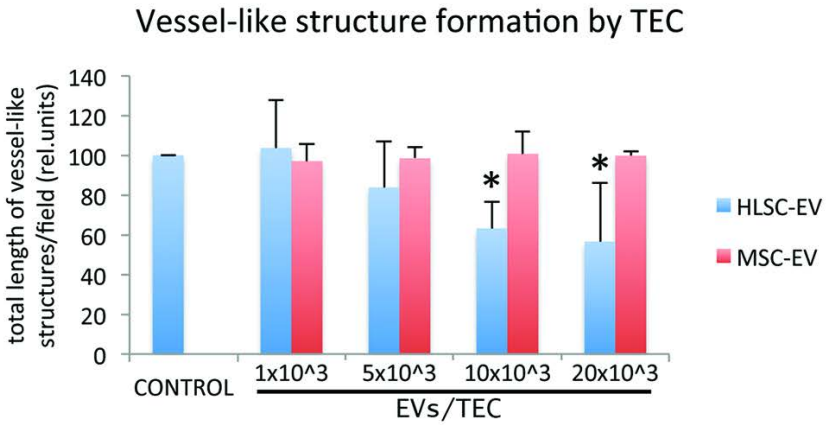

E

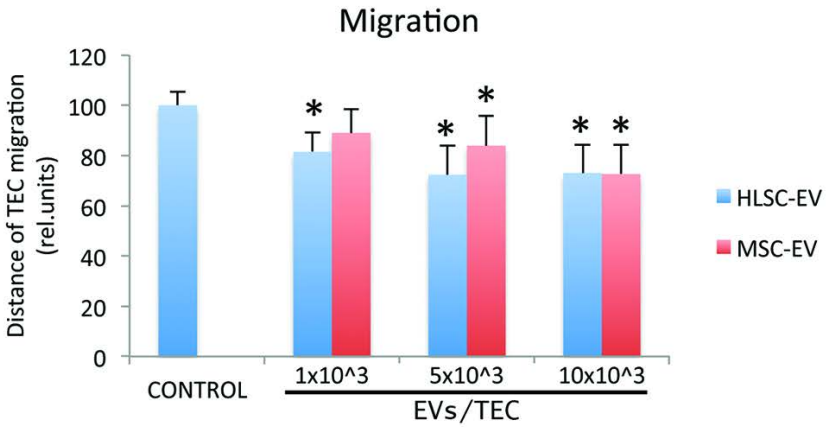

F

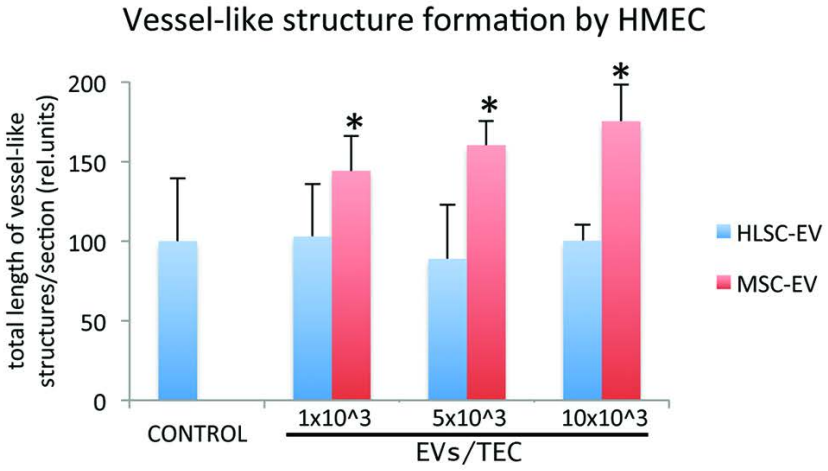

Figure 1

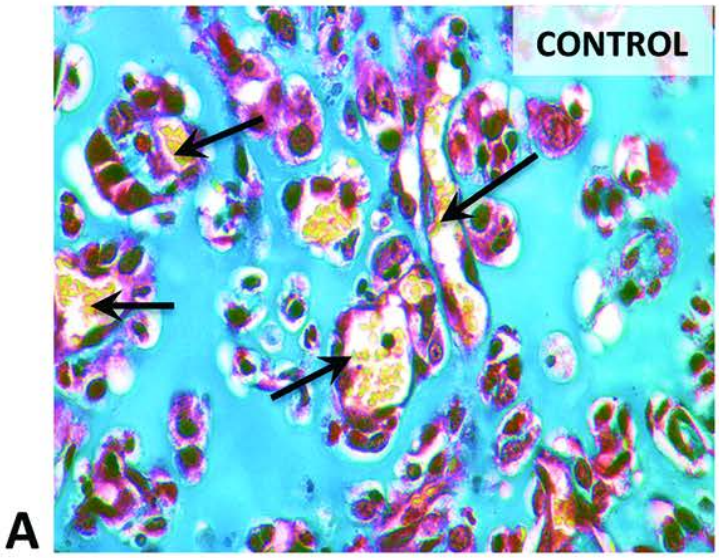

A

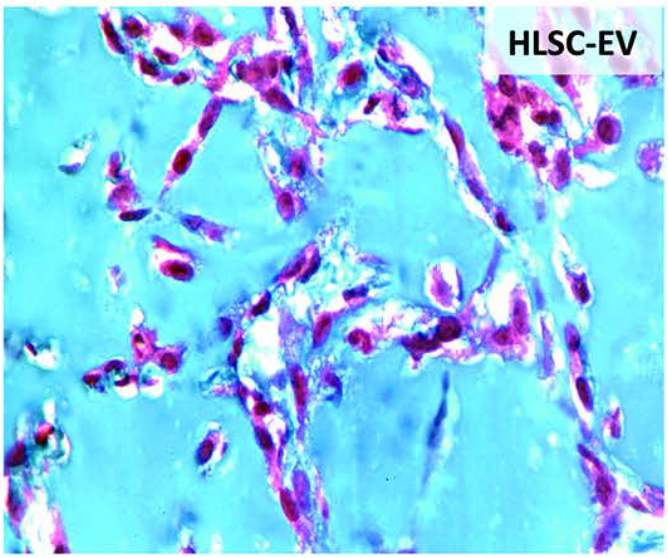

B

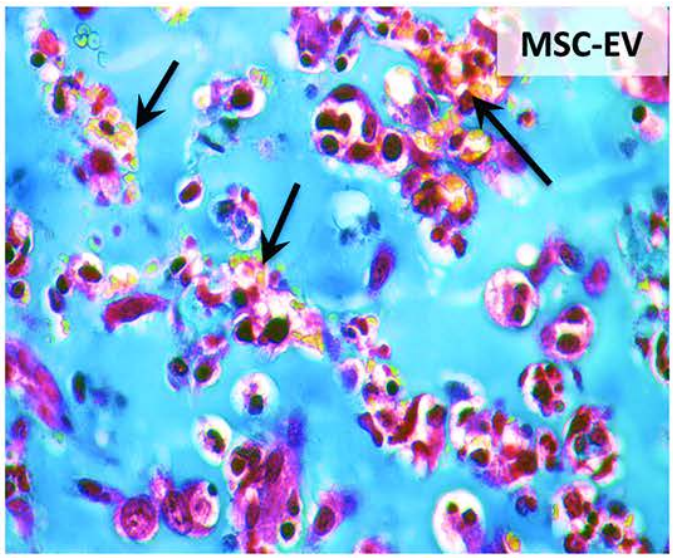

C

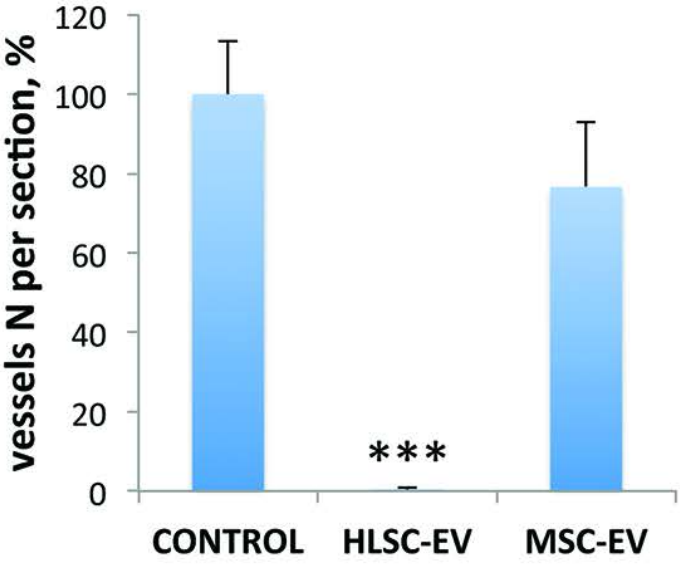

D

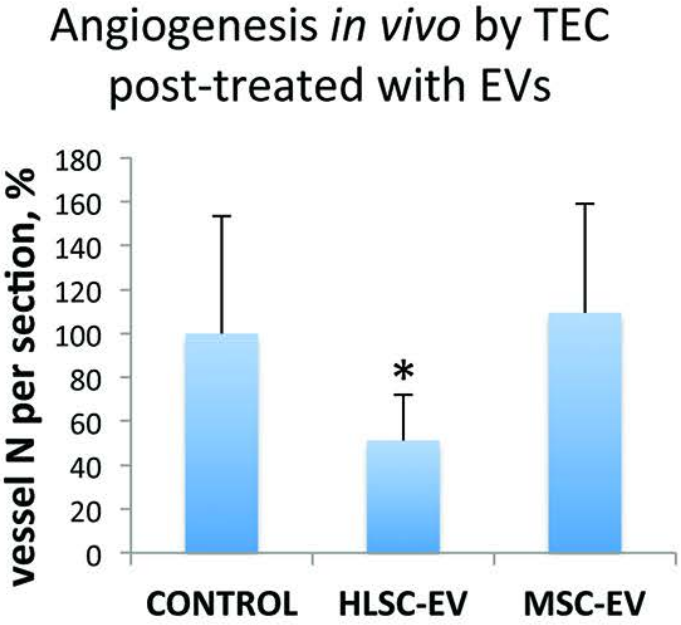

E

Figure 2

A

Gene	Fold Change	CI (95%)
TIE1	0,31	(0.00001, 0.68)
ITGB3	0,39	(0.04, 0.74)
FGF1	0,40	(0.00001, 0.88)
AKT1	0,41	(0.00001, 1.39)
F3	0,42	(0.00001, 1.44)
THBS1	0,42	(0.00001, 1.36)
TGFA	0,43	(0.00001, 1.34)
CCL11	0,45	(0.00001, 1.20)
EPHB4	0,45	(0.00001, 1.44)
PLAU	0,51	(0.02, 1.00)
TGFB1	0,53	(0.00001, 1.80)
ENG	0,55	(0.00001, 1.13)

B

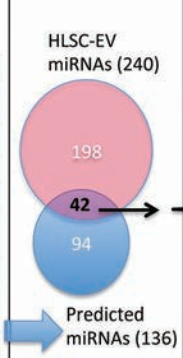

C

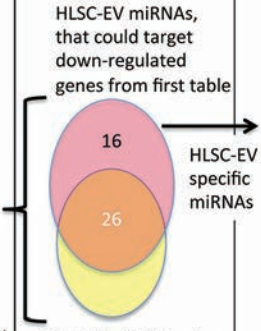

D

miRNAs		Genes
hsa-miR-30e-5p	Pro-tumorigenic	ITGB3
hsa-miR-320d	Tumor suppressor	
hsa-miR-320c	Tumor suppressor	
hsa-miR-424-5p	Anti-angiogenic	FGF1
hsa-miR-15a-5p	Anti-angiogenic	
hsa-miR-874-3p	Tumor suppressor	
hsa-miR-301a-3p	Pro-tumorigenic	F3
hsa-miR-93-5p	Anti-angiogenic	
hsa-miR-20b-5p	Anti-angiogenic	
hsa-miR-212-3p	Pro-tumorigenic	THBS1
hsa-miR-301a-3p	Pro-tumorigenic	TGFA
hsa-miR-23a-3p	Anti-angiogenic	
hsa-miR-23b-3p	Anti-angiogenic	
hsa-miR-20b-5p	Anti-angiogenic	EPHB4
hsa-miR-93-5p	Anti-angiogenic	
hsa-miR-181d-5p	Tumor suppressor	PLAU
hsa-miR-181b-5p	Tumor suppressor	
hsa-miR-181c-5p	Tumor suppressor	

Figure 3

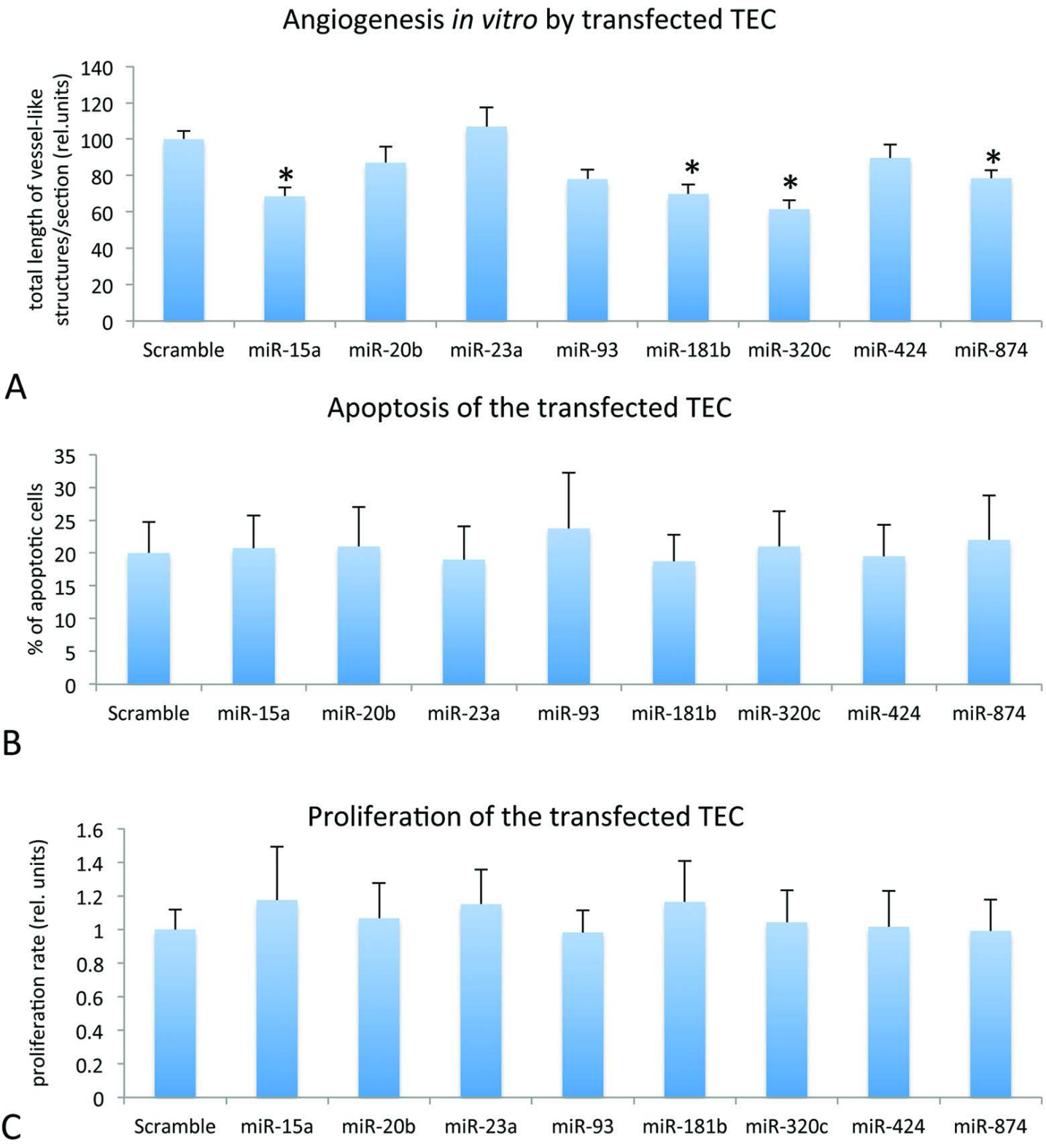
Angiogenesis *in vitro* by transfected TEC
total length of vessel-like structures/section (rel.units)
140
120
100
80
60
40
20
0
*
*
*
*
Scramble
miR-15a
miR-20b
miR-23a
miR-93
miR-181b
miR-320c
miR-424
miR-874
A
Apoptosis of the transfected TEC
% of apoptotic cells
35
30
25
20
15
10
5
0
Scramble
miR-15a
miR-20b
miR-23a
miR-93
miR-181b
miR-320c
miR-424
miR-874
B
Proliferation of the transfected TEC
proliferation rate (rel. units)
1.6
1.4
1.2
1
0.8
0.6
0.4
0.2
0
Scramble
miR-15a
miR-20b
miR-23a
miR-93
miR-181b
miR-320c
miR-424
miR-874
C

Figure 4

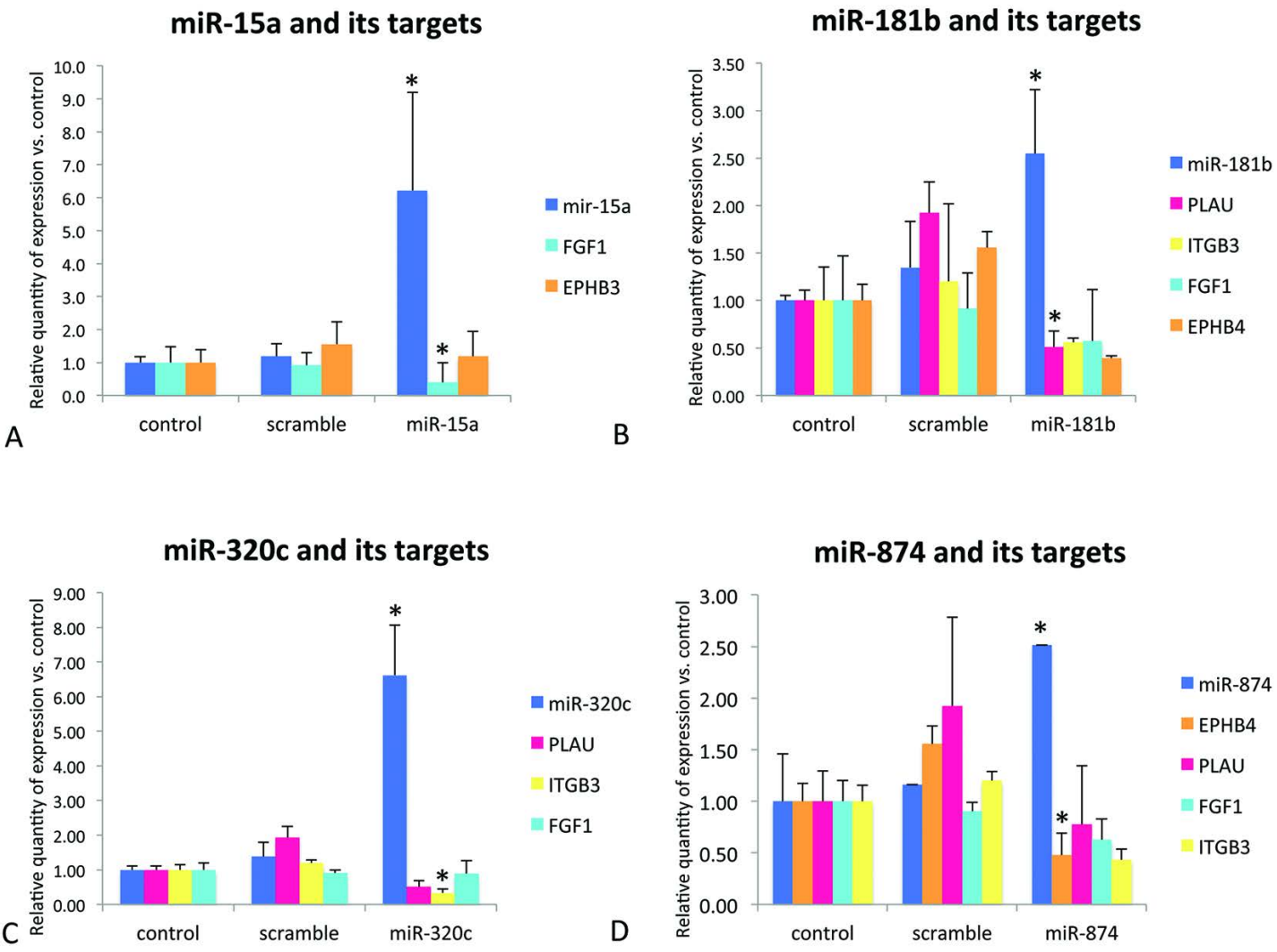
miR-15a and its targets
Relative quantity of expression vs. control
10.0
9.0
8.0
7.0
6.0
5.0
4.0
3.0
2.0
1.0
0.0
control
scramble
miR-15a
mir-15a
FGF1
EPHB3
A
miR-181b and its targets
Relative quantity of expression vs. control
3.50
3.00
2.50
2.00
1.50
1.00
0.50
0.00
control
scramble
miR-181b
miR-181b
PLAU
ITGB3
FGF1
EPHB4
B
miR-320c and its targets
Relative quantity of expression vs. control
9.00
8.00
7.00
6.00
5.00
4.00
3.00
2.00
1.00
0.00
control
scramble
miR-320c
miR-320c
PLAU
ITGB3
FGF1
C
miR-874 and its targets
Relative quantity of expression vs. control
3.00
2.50
2.00
1.50
1.00
0.50
0.00
control
scramble
miR-874
miR-874
EPHB4
PLAU
FGF1
ITGB3
D

Figure 5

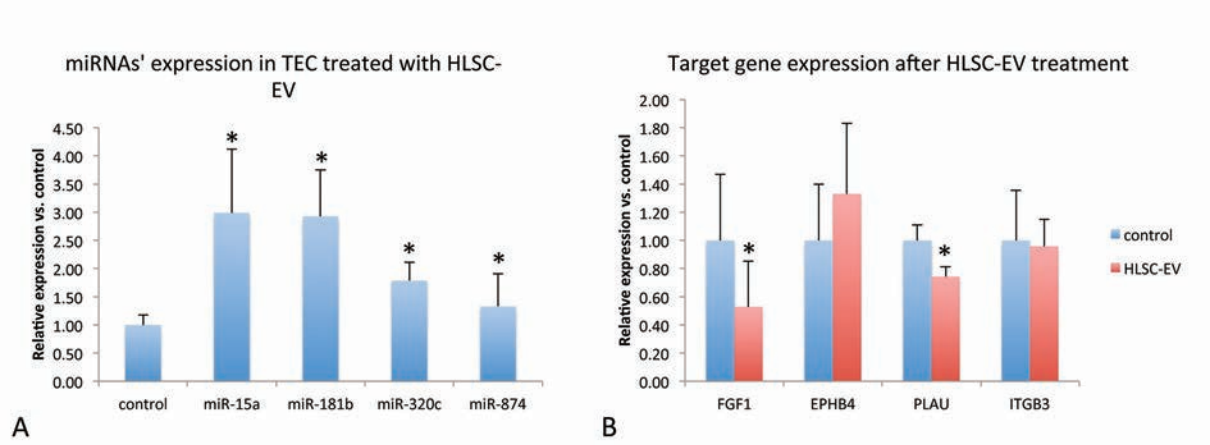
miRNAs' expression in TEC treated with HLSC-EV
Relative expression vs. control
4.50
4.00
3.50
3.00
2.50
2.00
1.50
1.00
0.50
0.00
control
miR-15a
miR-181b
miR-320c
miR-874
A
Target gene expression after HLSC-EV treatment
Relative expression vs. control
2.00
1.80
1.60
1.40
1.20
1.00
0.80
0.60
0.40
0.20
0.00
FGF1
EPHB4
PLAU
ITGB3
control
HLSC-EV
B
control
scramble
miR-15a
HLSC-EV
FGF1
C
control
scramble
miR-181b
HLSC-EV
PLAU
D

Figure 6